# Brief overview about Shear Wave Elastography and Sonographic abnormalities of Wrist and hand in rheumatoid patient

**Rania Mostafa Almolla, Hossam Eldin Mansour Abdelrahman, Rahma Hossam Abdelsalam, Nesma Adel Hamed**

Department of Radiodiagnosis, Faculty of Medicine, Zagazig University, Egypt

Email: Rahmahossam330@gmail.com

**Abstract**

**Background:** Shear wave elastography is a rapidly evolving US imaging technique that allows quantification of mechanical and elastic tissue properties and serves as an adjunct to conventional US techniques, aiding in initial characterization and treatment follow-up of various traumatic and pathologic conditions of the musculoskeletal system. In the past 2 decades, sonoelastography has been progressively used as a tool to help evaluate soft-tissue elasticity and add to information obtained with conventional gray-scale and Doppler ultrasonographic techniques. Recently introduced on clinical scanners, shear-wave elastography (SWE) is considered to be more objective, quantitative, and reproducible than compression sonoelastography with increasing applications to the musculoskeletal system. High resolution ultrasonography is an excellent and cost effective modality for early diagnosis of inflammatory arthritis. It detects mild synovitis when clinical examination is equivocal. The major abnormalities of RA appear in the synovial joints as soft tissue swelling caused by synovial hypertrophy, effusion, bursal and tendon sheath swelling. Marginal erosions are due to inflamed synovium destroying the cortex and underlying bone and they occur initially at the bare area: the margins where synovium is not covered by cartilage.

**Keywords:** Shear Wave Elastography, rheumatoid

## Introduction

Shear wave elastography is a rapidly evolving US imaging technique that allows quantification of mechanical and elastic tissue properties and serves as an adjunct to conventional US techniques, aiding in initial characterization and treatment follow-up of various traumatic and pathologic conditions of the musculoskeletal system. **(1)**.

In the past 2 decades, sonoelastography has been progressively used as a tool to help evaluate soft-tissue elasticity and add to information obtained with conventional gray-scale and Doppler ultrasonographic techniques. Recently introduced on clinical scanners, shear-wave elastography (SWE) is considered to be more objective, quantitative, and reproducible than compression sonoelastography with increasing applications to the musculoskeletal system **(1)**.

SWE uses an acoustic radiation force pulse sequence to generate shear waves, which propagate perpendicular to the ultrasound beam, causing transient displacements. The distribution of shear-wave velocities at each pixel is directly related to the shear modulus, an absolute measure of the tissue's elastic properties. Shear-wave images are automatically coregistered with standard B-mode images to provide quantitative color elastograms with anatomic specificity. Shear waves propagate faster through stiffer contracted tissue, as well as along the long axis of tendon and muscle. SWE has a promising role in determining the severity of disease and treatment follow-up of various musculoskeletal tissues including tendons, muscles, nerves, and ligaments. **(1)**. To simplify the explanation of the basic physics, the shear wave is a transverse wave that occurs in an elastic medium that is subject to a periodic shear force. Shear is

defined as change in the shape of a substance layer without volume change, produced by a pair of equal forces working in opposite directions along the two opposed sides of the layer. After the shear interaction, the initial layer (tissue) will resume its original shape, while the adjacent layers undergo shear, and there will be further shifting of the shear wave, which propagates as a transverse shear wave **(1)**.
For a better understanding of SWE shear-wave elastography.
we will describe it in three simple steps,. In step 1, *shear waves are generated using focused acoustic radiation force from a linear US array, which by itself provides a local stress and generates local displacement in the tissue.*

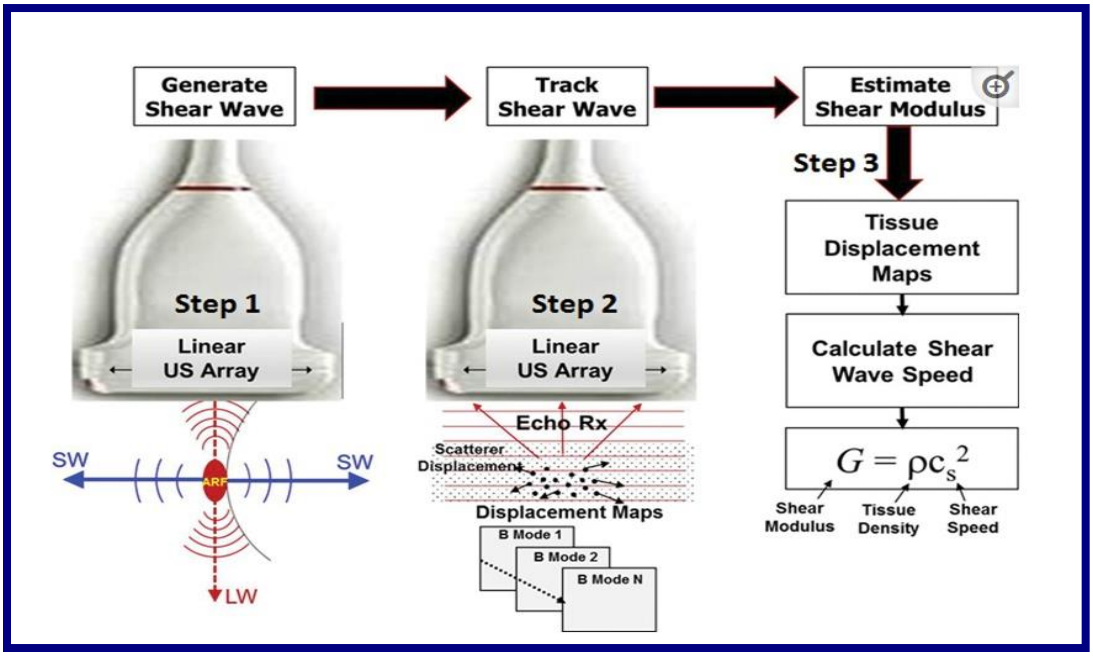


**Fig. (1) . (a)** Basic physics of SWE shear-wave elastography. In step 1, shear waves are generated using acoustic radiation force; they propagate perpendicularly to the primary US wave at a lower velocity. In step 2, fast plane wave excitation is used to track displacement and velocity as shear waves propagate, and tissue displacement is calculated using a speckle tracking algorithm. In step 3, tissue displacements are used to calculate shear-wave velocity (*c*s) and shear modulus *(G)*. **(b)** Relationship between shear velocity and shear modulus expressed as a color bar, which assumes, in this case, a density equal to that of water (1 g/cm3). Actual density estimates will vary for different types of soft tissue and can also be found using values published in the literature. **(1)**.
Generated shear waves then propagate through the adjacent tissues in the transverse plane, perpendicular to the primary wave that produces the acoustic radiation force, at a much slower velocity, causing shear displacements in tissue. **(2).**
In step 2, fast plane wave excitation is used to track the tissue displacement and shear wave velocities as the shear waves propagate. Tissue displacement is calculated using a speckle tracking algorithm **(1)**.

In step 3, tissue displacement maps are used to calculate shear-wave velocity ($c_s$), frequently expressed in meters per second. The distribution of shear-wave velocities at each pixel is directly related to the shear modulus *G*, which is calculated by a simple mathematical equation and expresses the tissue stiffness and elasticity in units of pressure normally kilopascals. The shear modulus is defined as the ratio of stress to strain that is given by $G = \rho c_s^2$, where ρ is the material density. The Young modulus (*E* [or λ]) is defined to be $E = 3G$ for isotropic media. The material density for soft tissue is typically estimated on the basis of values published in the literature for the type of tissue being examined, or approximated to be close to that of water (1 g/cm$^3$) **(1)**.
Note that there is a direct relationship between the shear and the young moduli, reported in some studies to be $E = 2G(1+\upsilon)$, where υ is the Poisson ratio. Because soft tissues with small deformations (ie, quasi-static displacements) are usually assumed to be incompressible (ie, $\upsilon = 0.5$), *G* is sometimes converted to *E* by the

simple equation $E = 3G$ for incompressible media **(3).** Therefore, although some studies refer to shear-wave values or to $G$, others report $E$ on the basis of this relationship. *On the US screen, quantitative shear modulus maps are represented in a color-coded elastogram displaying shear-wave velocities in meters per second or tissue elasticity in kilopascals* (**4).** For the color elastograms, red is usually defined for encoding hard consistency, blue indicates soft consistency, and green and yellow encode intermediate stiffness. Understanding and interpreting color elastograms and shear-wave velocities requires knowledge of the basic ultrasound physics of SWE shear-wave elastography. In comparison with compression sonoelastography, SWE shear-wave elastography is considered to be more objective and reproducible and allows direct assessment of tissue elasticity, with the possibility to obtain quantitative measurements without the need for manual compression **(4).**

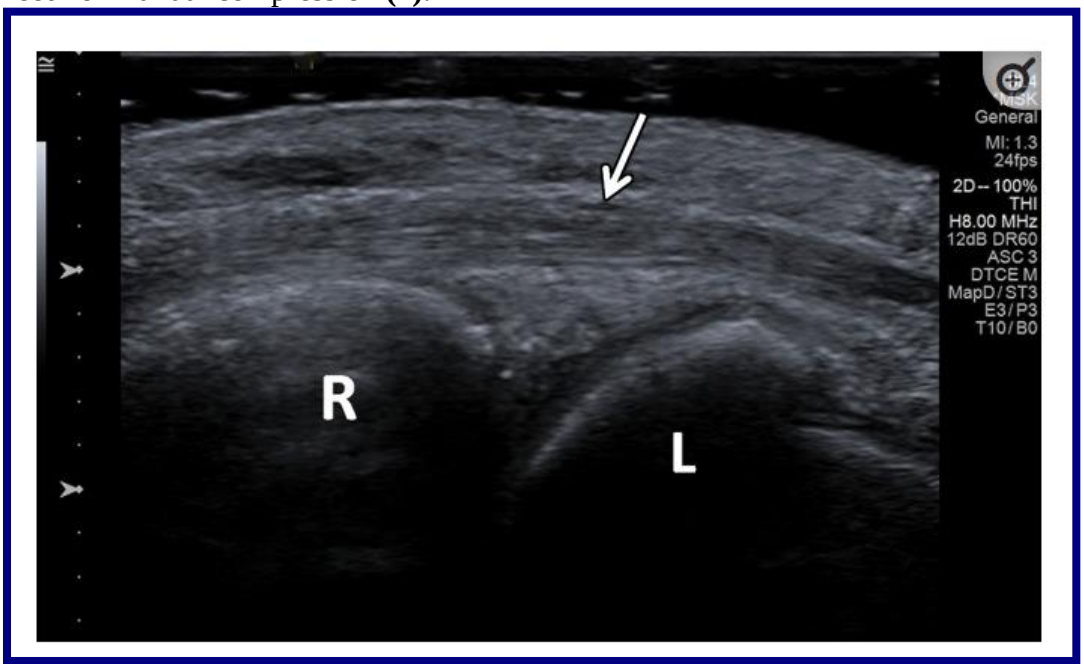


**Figs. (2)** Normal fourth extensor compartment tendon of the wrist in a 21-year-old asymptomatic man. **(a)** Long-axis gray-scale US image of the dorsal aspect of the wrist shows a normal echogenic fibrillar appearance of the fourth extensor compartment tendon (arrow). *L* = lunate, *R* = radius. **(b)** SWE shear-wave elastography image (color elastogram) of the same region shows predominantly intermediate shear-wave velocity (6.66 m/sec) in the same tendon (arrow). Red = hard consistency (≤15 m/sec), blue = soft consistency (≥0.5 m/sec), and green and yellow = intermediate consistency. SWE shear-wave elastography data were collected using an Acuson S3000 US scanner (Siemens Healthineers, Erlangen, Germany) with a L9–4-MHz linear transducer. **(4).**

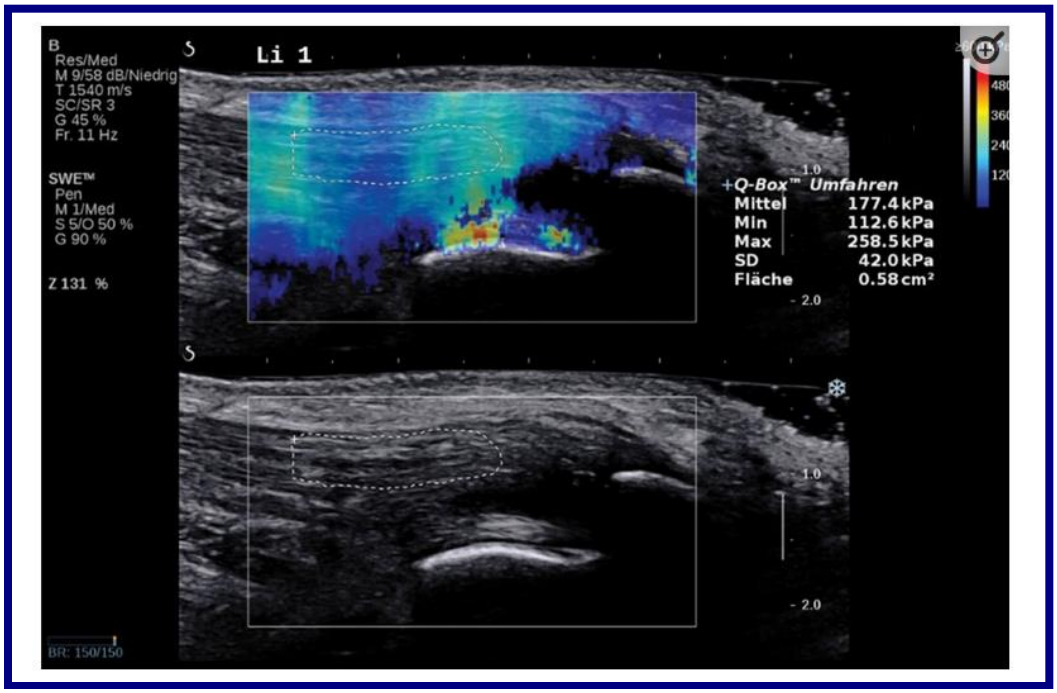


**Figs. (3)** Normal Achilles tendon in a 69-year-old asymptomatic woman. Bottom image: Long-axis gray-scale US image shows normal echogenic fibrillar appearance of the Achilles tendon with an outlined region of interest (ROI). Top image: Color elastogram of the same region shows normal *G* of the examined tendon (177.4 kPa ± 42). SWE shear-wave elastography data were collected using an Aixplorer US scanner (Supersonic Imagine, Aix-en-Provence, France) with an L15–4-MHz linear transducer. **(4).**

Shear waves travel through soft tissues approximately 1000 times slower and attenuate approximately 10 000 times faster than longitudinal conventional ultrasound waves. Their passage, including their speed, can be observed on US images as long as the ultrasound echoes can be generated frequently enough **(3).**

Frame rates for tracking shear waves are typically between 2 kHz and 10 kHz. A quality index is often displayed to the sonographer as a measure of confidence of the shear wave estimate. The quality index is related to the correlation coefficient for tracking the shear displacements. If the frame rate is too low or there is no developed speckle in the region (eg, from fluid), the quality index is low (below a user-defined threshold of about 0.9) and the shear-wave elastogram displays a signal void (no estimate for shear-wave velocities at that region) **(2).**

A signal void in superficial structures is usually due to the presence of fluid (eg, edema, blood) and may provide additional diagnostic information. **(2).**

A primary limitation of SWE shear-wave elastography is depth of penetration. Shallow depths may be accommodated by applying a 5-mm layer of coupling US gel as standoff. The shape and size of the ROI region of interest for postanalysis is also limited on some scanners. Most scanners require a timeout of a few seconds before the next acquisition, which prevents real-time dynamic imaging of structures in motion. Additionally, SWE shear-wave elastography is sensitive to transducer pressure and angle, and the shear modulus depends on the orientation of the probe relative to the examined structures **(2).**

**Sonographic abnormalities of Wrist and hand in rheumatoid patient**

High resolution ultrasonography is an excellent and cost-effective modality for early diagnosis of inflammatory arthritis. It detects mild synovitis when clinical examination is equivocal **(5).**

High resolution ultrasonography reliably differentiates between synovitis and other causes of joint swelling, such as subcutaneous oedema and tenosynovitis **(5).**

It is accurate for detecting joint effusion and synovial hypertrophy and more objective qualitative and quantitative assessment of synovitis can be obtained with presently available equipments **(5).**

**Sonographic Abnormalities in Ra**

The major abnormalities of RA appear in the synovial joints as soft tissue swelling caused by synovial hypertrophy, effusion, bursal and tendon sheath swelling **(5).**

Marginal erosions are due to inflamed synovium destroying the cortex and underlying bone and they occur initially at the bare area: the margins where synovium is not covered by cartilage **(5).**

**1- Synovitis**

The synovial membrane covers the inner surface of articular cavity and its recesses, the bursae, and the tendon sheaths. Synovial inflammation produces oedema and stimulates hyper secretion by the membrane. **(6)**

On grey scale synovial hypertrophy appears as hypoechoic thickening within the joint**.** Graded compression of an articular recess evacuates its fluid and allows detection of hypertrophic synovium. Increased synovial vascularity is usually seen in active inflammation on power Doppler**.** Low resistive index (RI) on pulsed spectral Doppler may serve as an objective marker of disease activity. **(6)**

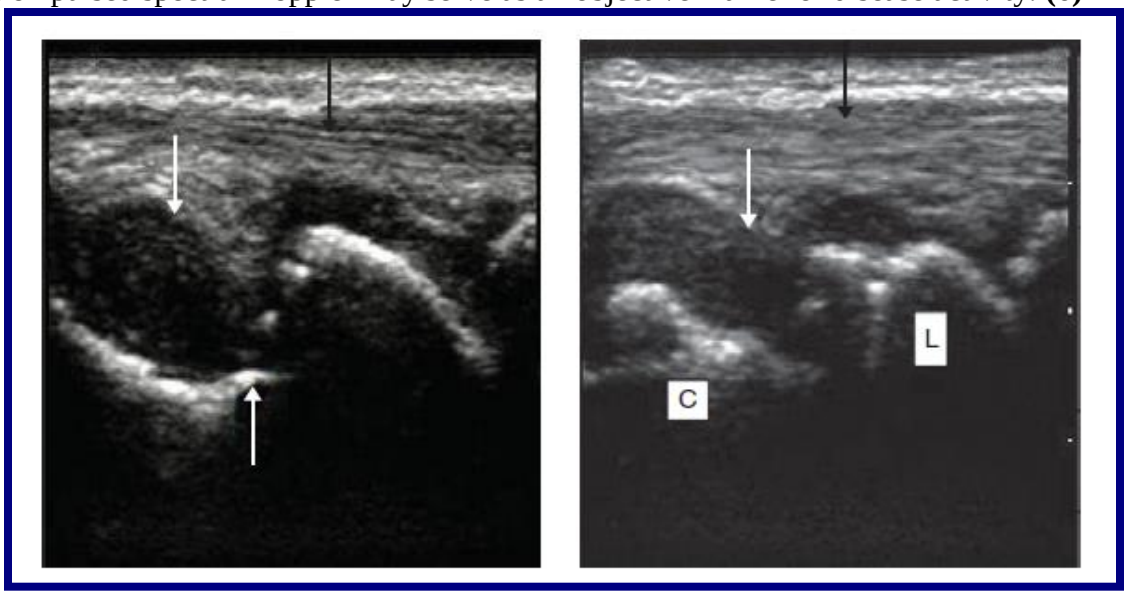


**Fig. (4).** Longitudinal image of radio-carpal joints showing hypoechoic synovial hypertrophy (white arrows). Normal bright undulating surface of carpal bones (small solid arrow). L = Lunate, C = Capitate. Normal extensor tendon (black arrows). **(6)**

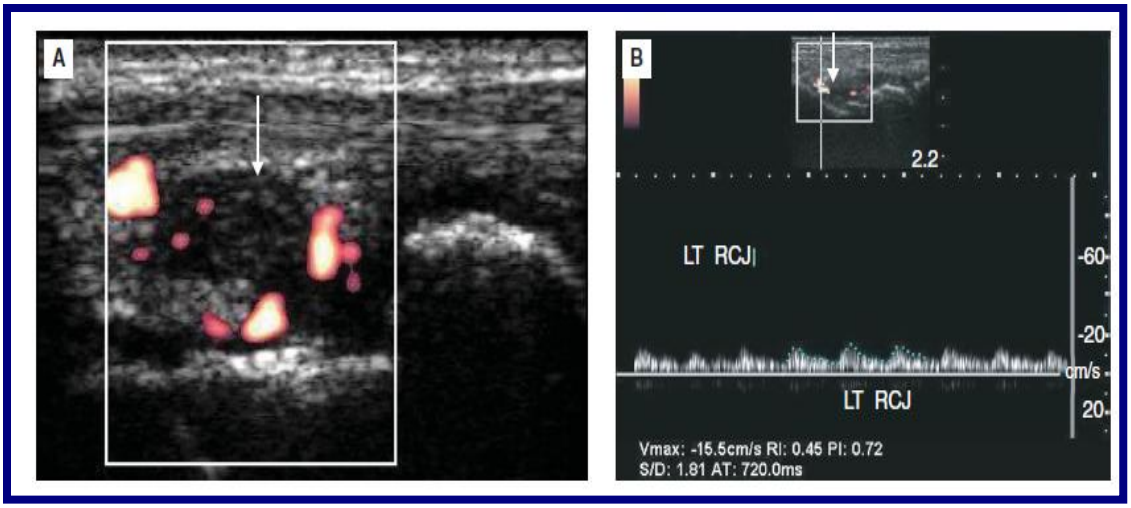


**Fig. (5).** Longitudinal image of the radio-carpal joint on power Doppler showing moderately increased synovial vascularity (image A, white arrow). B Spectral Doppler tracing showing low resistance flow (RI-0.45) suggestive of active inflammation. **(6)**

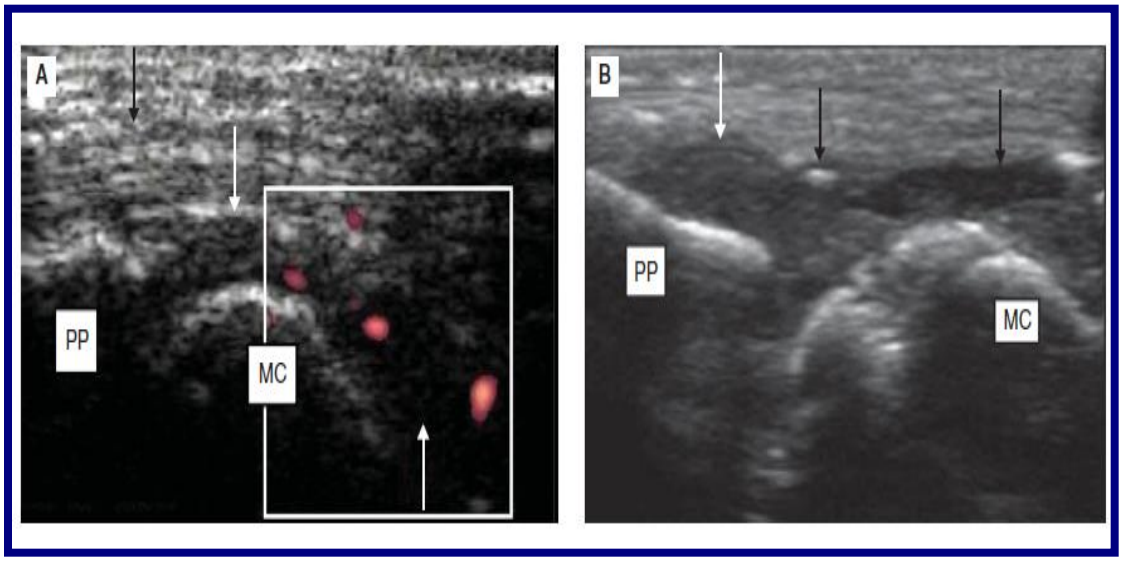


**Fig. (6).** Flexor aspect of MCP joint showing hypoechoic synovial hypertrophy with moderately increased vascularity on power Doppler (image A, white arrow). Distended proximal recess (small arrow). Normal flexor tendon (black arrow). B Longitudinal image of flexor aspect of MCP joint after US guided intra-articular steroid injection. Synovial hypertrophy (white arrow). Injected fluid (long black arrow). Echogenic air bubble (small black arrow). MC = metacarpal, PP = proximal phalanx**. (6)**

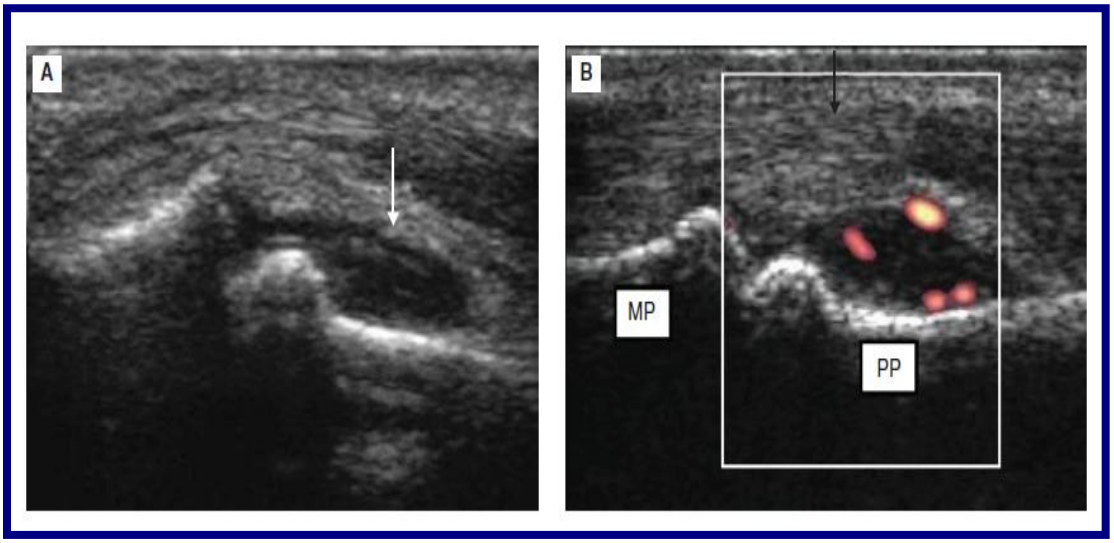


**Fig. (7).** Longitudinal image of flexor aspect of PIP joint showing hypoechoic synovial hypertrophy distending the synovial recess (Image-A, white arrow). B Moderately increased vascularity on power Doppler. PP = proximal phalanx, MP = middle phalanx. Flexor tendons (black arrow). **(6)**

**2- Effusion**

On sonograms joint effusion typically appears anechoic**.** However posterior enhancement is rarely seen because of presence of underlying bony structures. The fluid is typically displaced on graded transducer compression. Septations and internal echoes can be seen within the joint fluid. Larger echogenic structures may represent blood
clots, fibrinous deposits or synovial masses. USG is not able to distinguish reliably the exact nature of fluid and joint aspiration remains essential for diagnosis. **(6)**

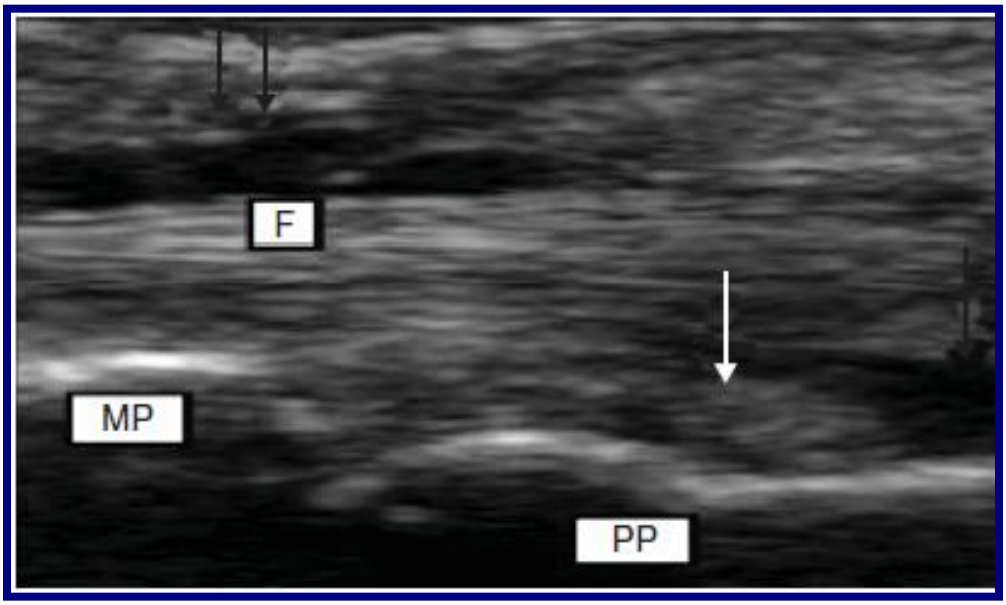


**Fig. (8).** Longitudinal image of flexor aspect of PIP joint showing synovial hypertrophy (white arrow) and anechoic effusion (single black arrow). F = flexor tendon, fluid in tendon sheath (double black arrow). PP = proximal phalanx, MP = middle phalanx. **(6)**

### 3- Tenosynovitis

The synovial membrane of a tendon sheath is histologically identical to that of the diarthrodial joints. Inflammation of tendon sheath's synovial membrane induces oedema with fluid accumulation in the tendon sheath. On greyscale sonograms, the tendon appears as a central hyper echoic structure with a hypoechoic halo of effusion, synovial thickening or pannus**.** Increased vascularity may be seen around the tendon on power Doppler in active inflammation**. (6)**

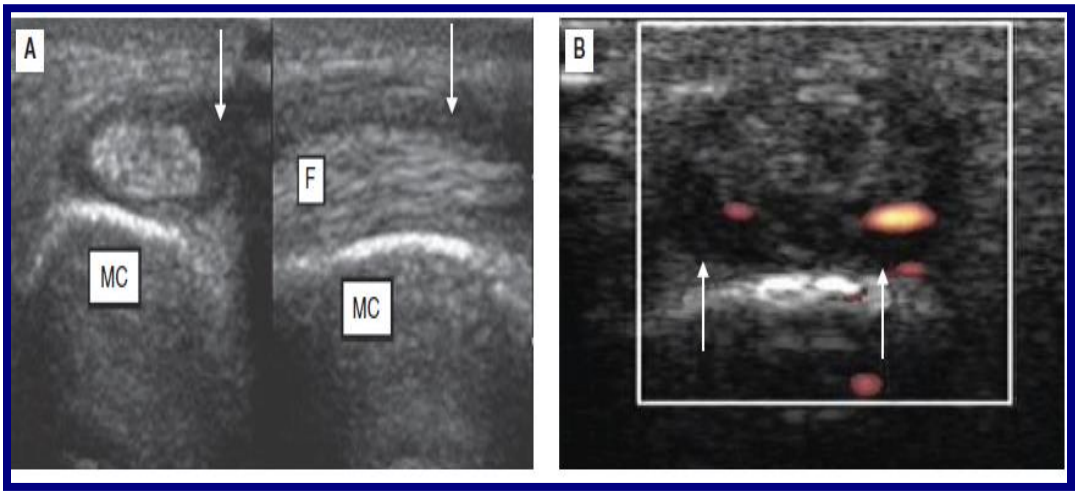


**Fig. (9). A** Transverse and longitudinal image on flexor aspect of MCP joint showing hypoechoic synovial thickening (white arrows) surrounding the echogenic flexor tendon (F) to second digit consistent with tenosynovitis. MC = metacarpal (image-A). **B** Transverse image showing increased vascularity on power Doppler. **(6)**

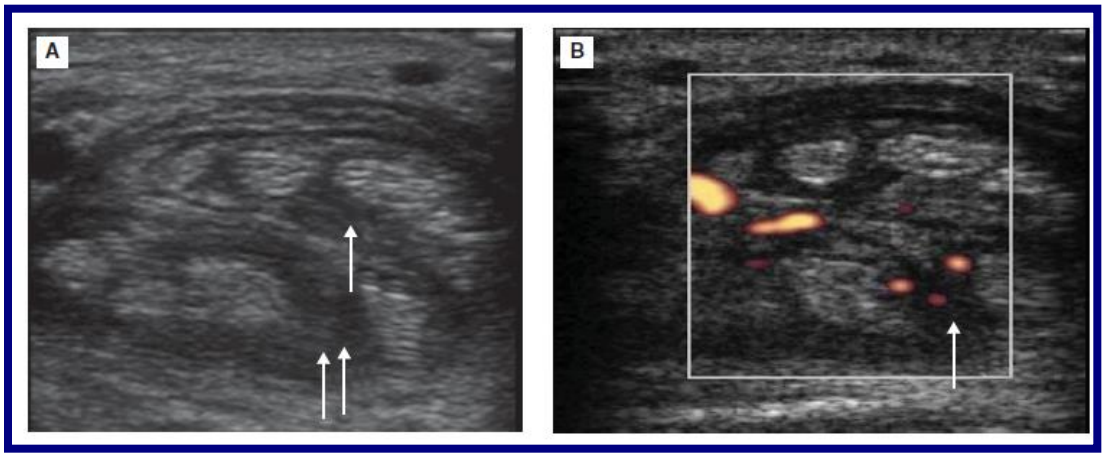


**Fig. (10). A** Transverse image at carpal tunnel showing hypoechoic synovial hypertrophy (white arrows) surrounding the flexor digitorum superficialis (single arrow) and flexor digitorum profundus tendons (double arrow) consistent with tenosynovitis. **B** Transverse scan showing increased vascularity on power Doppler**. (6)**

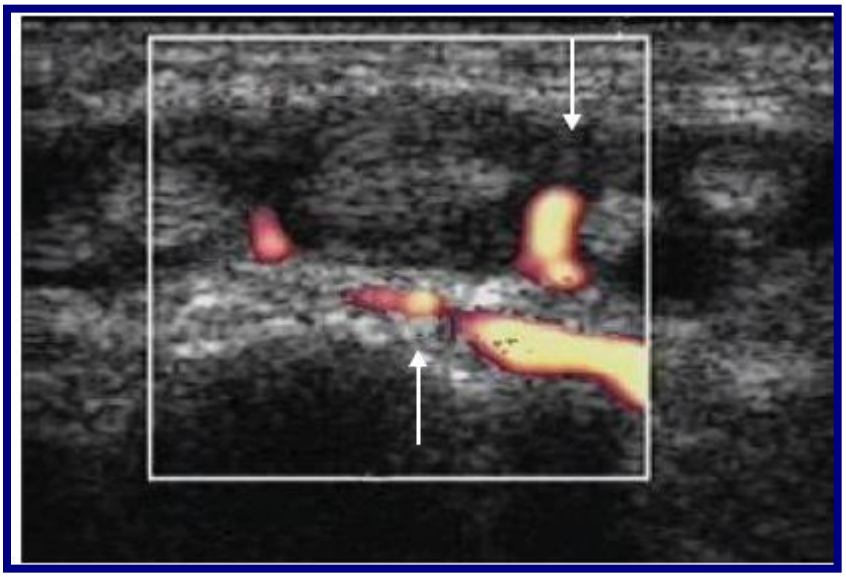

**Fig. (11)** .Transverse image at dorsal wrist showing hypoechoic synovial thickening (upper white arrow) surrounding extensor digitorum tendons (compartment IV) with increased vascularity on power Doppler (lower arrow). **(6)**

### 4- Erosion

Normal cortical bone appears as a smooth essentially perfect specular reflector seen as linear echogenic shadow. Erosion is seen as an irregular floored defect in the bone cortex visualized in both longitudinal and transverse planes to exclude artifactual pseudo artifacts produced by suboptimal angulation of the transducer**.** In RA, pannus is seen as hypoechoic soft tissue filling these erosions. Power Doppler usually shows an increase in vascularity at these sites especially in active disease. In acutely inflamed jointswith erosions, a vascular pedicle may be seen supplying the pannus up to the erosion crater ***(*6)**

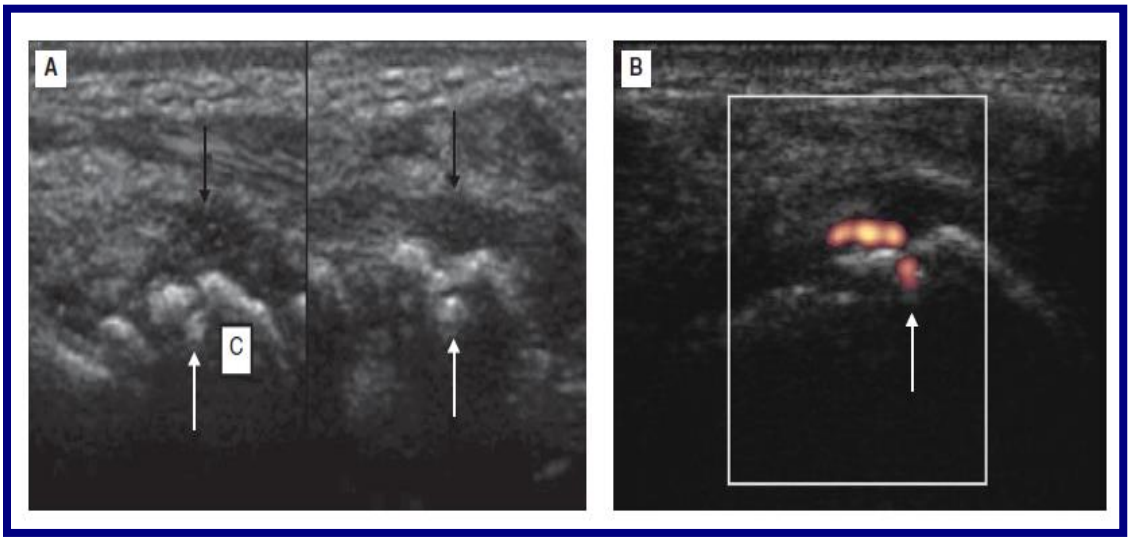


**Fig. (12). A** Longitudinal and transverse image of radio-carpal joints showing hypoechoic synovial hypertrophy (black arrows) overlying the erosions (white arrows) seen as cortical defects. **B** Longitudinal image showing erosion with supplying vascular pedicle on power Doppler (white arrow). **(6)**

### 5- Other findings

Rheumatoid nodules appear as small well defined, hypoechoic oval areas in peri-articular soft tissues. Ganglion cysts and carpal tunnel syndrome are other commonly seen findings. **(6)**

**Assessment of disease activity**

Disease activity assessment in RA is essential for therapeutic decisions, outcome assessment and monitoring response to treatment. Clinical assessment, laboratory parameters and radiographic findings are routinely used to evaluate the disease activity. Musculoskeletal USG is now playing an increasingly important role in the evaluation of disease activity in RA due to its ability to detect sub-clinical synovitis. Moreover colour.

Doppler and power Doppler demonstrates synovial and tenosynovial neovascularity as a measure of inflammation **(7).**

Various scoring systems have been used for evaluation of synovitis to increase the reproducibility and validity of USG. Qualitative, semi-quantitative and quantitative greyscale and Doppler methods have been used for evaluating rheumatoid joint inflammation. **(8,9).**

Semi-quantitative scoring of synovitis and power Doppler signal in rheumatoid joints is easily applicable in clinical practice and offers good inter-observer and inter-machine reliability. Quantitative assessment of synovial thickness or synovial Doppler signal is more sensitive to change as compared to semi quantitative method. In quantitative Doppler scoring system computer-assisted measurement of colour pixels is done in a specific area of interest along with Spectral Doppler analysis and measurement of resistive index. Low values of resistive index are obtained in areas of low resistance flow indicating inflammation. These Doppler parameters are reliable and give insight into the disease pathophysiology making them important research tools. However, they are time consuming and probably not feasible in clinical practice. **(8,9).**

**Monitoring response to therapy**

There is now increasing evidence in RA that early identification and suppression of synovitis limits the progression of the disease improving the long term prognosis **(10).** Grey scale ultrasound can assess response of synovial inflammation to treatment in RA. **(10).**

It has added value over clinical examination and has been increasingly used to monitor therapy. Changes in synovial vascularity are earliest to appear independent of the type of treatment used. Changes in synovial volume are slower to respond, and measurable differences may take some time to appear in larger joints. Evidence of relation between early improvement in synovitis detected by USG and a reduction in radiographic findings in later years has been demonstrated. A number of longitudinal studies have shown a

significant improvement in joint inflammation evaluated by greyscale and Doppler USG, associated with clinical and laboratory response to therapy in RA patients treated with different drugs **(11,12).**
Sub-clinical synovitis can be detected by greyscale and PDUS in a high number of RA patients in clinical remission treated with disease-modifying anti-rheumatic drugs indicating true disease status **(13).** Preliminary results also indicate a predictive value of Doppler USG findings in RA outcome **(14,15).**

**Conflicts of Interest:** The authors declare no conflict of interest.

## References

1. **Taljanovic MS, Gimber LH, Becker GW, Latt LD, Klauser AS, Melville DM et al., (2017).** Shear-Wave Elastography: Basic Physics and Musculoskeletal Applications. Radiographics. ; 37(3):855-870.
2. **Bercoff J, Tanter M and Fink M. (2004).** Supersonic shear imaging: a new technique for soft tissue elasticity mapping. IEEE Trans Ultrason Ferroelectr Freq Control; 51(4):396–409.
3. **Wells PN and Liang HD. (2011).** Medical ultrasound: imaging of soft tissue strain and elasticity J R Soc Interface; 8(64):1521–1549.
4. **Li Y and Snedeker JG. (2011).** Elastography: modality-specific approaches, clinical applications, and research horizons. Skeletal Radiol; 40(4): 389–397.
5. **Gibbon WW and Wakefield RJ. (1999).** Ultrasound in inflammatory disease. Radiol Clin North Am; 37: 633–51.
6. **Banwari Sharma, Meenakshi Sharma (2009).** Ultrasonography of hands in rheumatoid arthritis Indian Journal of Rheumatology,(4):102–111.
7. **Wakefield RJ, Gibbon W, Conaghan P. G, O'Connor P, McGonagle, D, Pease C. T et al., (2000).** The value of sonography in the detection of bone erosions in patients with rheumatoid arthritis: A comparison with conventional radiography. Arthritis & Rheumatism, 43 (12), 2762–2770.
8. **Karim Z, Wakefield RJ, Quinn M, Conaghan PG, Brown AK, Veale DJ, et al., (2004).** Validation and reproducibility of ultrasonography in the detection of synovitis in the knee. Arthritis Rheum; 50: 387–94.
9. **Ellegaard K, Torp-Pedersen S and Bliddal H. (2008).** Quantification of color Doppler activity in the wrist in patients with rheumatoid arthritis. The reliability of different methods for image selection and evaluation. Ultraschall Med; 29: 393–8.
10. **Emery P. (1995).** Therapeutic approaches for early rheumatoid arthritis. How early? How aggressive? Br J Rheumatol; 34: 87.
11. **Ribbens C, André B, Marcelis S, Kaye O, Mathy L, Bonnet V, et al., (2003).** Rheumatoid hand joint synovitis: gray-scale and power Doppler US quantifications following anti-tumor necrosis factor-treatment: pilot study. Radiology; 229: 562–9.
12. **Naredo E, Bonilla G, Gamero F, Uson J, Carmona L and Laffon A. (2005)**. Assessment of inflammatory activity in rheumatoid arthritis: a comparative study of clinical evaluation with grey-scale and power Doppler ultrasonography. Ann Rheum Dis; 64: 375–81.
13. **Ozgocmen S, Ozdemir H, Kiris A, Bozgeyik Z and Ardicoglu O. (2008).** Clinical evaluation and power Doppler sonography in rheumatoid arthritis: evidence for ongoing synovial inflammation in clinical remission. South Med J; 101: 240–5.
14. **Taylor PC, Steuer A, Gruber J, Cosgrove DO, Blomley MJ, Marsters PA, et al., (2004).** Comparison of ultrasonographic assessment of synovitis and joint vascularity with radiographic evaluation in a randomized, placebo-controlled study of infliximab therapy in early rheumatoid arthritis. Arthritis Rheum 2004; 50: 1107–16.
15. **Brown A S, Quinn MA, Karim Z, Conaghan PG, Peterfy C., Hensor, E et al., (2006).** Presence of significant synovitis in rheumatoid arthritis patients with disease-modifying antirheumatic drug–induced clinical remission: Evidence from an imaging study may explain structural progression. Arthritis & Rheumatism, 54(12), 3761–3773.